

# Development of Mid-IR waveguides to implement high resolution spectrometers in integrated optics

Myriam Bonduelle<sup>a</sup>, Guillermo Martin<sup>a</sup>, Alain Morand<sup>b</sup>, Javier R. Vazquez de Aldana<sup>c</sup>,  
Carolina Romero Vázquez<sup>c</sup>, Nadège Courjal<sup>d</sup>, and Antoine Coste<sup>d</sup>

<sup>a</sup>Univ. Grenoble Alpes, CNRS, IPAG, 38000 Grenoble, France

<sup>b</sup>Univ. Grenoble. Alpes, Univ. Savoie Mont Blanc, CNRS, Grenoble INP\*, IMEP-LAHC,  
38000, Grenoble, France, \*Institute of Engineering Univ. Grenoble Alpes

<sup>c</sup>Grupo de Investigación en Aplicaciones del Láser y Fotónica (ALF-USAL), Facultad de  
Ciencias, Universidad de Salamanca, E-37008 Salamanca, Spain

<sup>d</sup>FEMTO-ST, Univ. Franche-Comté, CNRS, 15B avenue des Montboucons, F-25030,  
Besançon, France

## ABSTRACT

This work aims to present a new miniature spectrometer in the mid InfraRed (L Band), using the SWIFTS (Stationary Wave Integrated Fourier Transform Spectrometer) technology. A stationary wave obtained by injecting light on both sides of a channel waveguide (Gabor configuration) is sampled using nano-scattering centres (grooves) on the surface of the waveguide. A single groove per scattering centre will radiate the sampled signal with wide angular distribution, which is not compatible with the buried detection area of infrared detectors, resulting in crosstalk between pixels. An implementation of multiple grooves (antenna) for each sampling centre is proposed as a solution to improve directivity towards the detector pixel by narrowing the scattering angle of the extracted light. Here, the results are obtained using a Lithium Niobate ( $LiNbO_3$ ) substrate, as its electro-optic properties allow for an active modulation of the phase, and the technology explored is Direct Laser Writing, that allows to have buried 3D waveguides and nanogrooves. In order to integrate the detector in the device, different configurations are explored so as to obtain a robust and high-resolution device useful mainly for astronomical applications such as spectro-interferometry.

**Keywords:** Spectro-interferometry; Exo-zodiacal dust; Jupiter-like exoplanets; Miniature spectrometer; L-band; Lithium Niobate, Direct Laser Writing

## 1. INTRODUCTION

SWIFTS is based on the sampling of a stationary wave using nanoscattering centres on the surface of a waveguide. Typically, the stationary wave is obtained with a mirror set at the end of the waveguide (Lippmann configuration). Although simpler in principle to achieve, the stationary wave obtained is a half-wide band interferogram, necessarily symmetric, hiding important information of the source (i.e. chromatic dispersion effects). Here, a Gabor configuration is proposed : the incoming light is divided before entering the sample, and injected on both sides of the waveguide, allowing the obtention of a complete wideband interferogram <sup>1</sup> The technology used, Direct Laser Writing (DLW), allows to simultaneously fabricate the waveguides and the 3D buried nanogrooves, enabling complex configurations and high precision on the nanometric size and position of the gratings. The samples presented here are made in Lithium Niobate, a birefringent crystal that allows a better sampling of the interferogram thanks to its electro-optics properties. Although the SWIFTS Lippman has been largely validated in the visible, due to the deeply buried detection area on the IR detectors, the diffracted signal obtained with a unique scattering centre is too wide and causes pixel crosstalk. Therefore, several nanogrooves per scattering centre are implemented, in order to act as a small grating and reduce the angular divergence of the extracted

---

Further author information: (Send correspondence to M. B.)  
M. B. : E-mail: myriam.bonduelle@univ-grenoble-alpes.fr

flux, reducing crosstalk and increasing the sampled intensity, therefore increasing the SNR 2. With these directive antenna, the final step to obtain a compact, monolithic spectrometer, is to have the detector’s pixel matrix bonded to the sample. This hybridization approach will be explored, as well as an alternative that is to directly grow the pixel on the surface of the sample, some  $\mu\text{m}$  above the antennas. Combined with the SWIFTS principle, DLW allows for a compact, robust and high- resolution spectrometer, useful notably for astronomical applications. Furthermore, the L-band ( $3.4 \mu\text{m} - 4.1 \mu\text{m}$ ) presents several key characteristics that are interesting in astrophysics. In this wavelength range, the atmosphere is relatively transparent, allowing for a better SNR ratio. Additionally, this band is useful for the exploration of the environment of young stars, as well as the detection of exo-zodiacal dust 3.

## 2. THEORETICAL BACKGROUND

### 2.1 SWIFTS’S principle

The optical beam is injected on both sides of a single-mode planar waveguide, creating a stationary interferogram with a period of  $\Lambda = \frac{\lambda}{2n}$ . The interferogram is then sampled by the nanoscattering centres (di-electric discontinuities), periodically placed in the evanescent field of the stationary wave. These centres are carefully made in order to create a default in the sample that will allow the light to radiate outside the waveguide, but without extracting too much of the flux. The radiated light is then imaged on a detector set very close to the sample’s surface (see fig1). Finally, using the discrete and periodical sampled values of the interferogram, through a Fourier Transform, the spectrum of the source can be reconstructed.

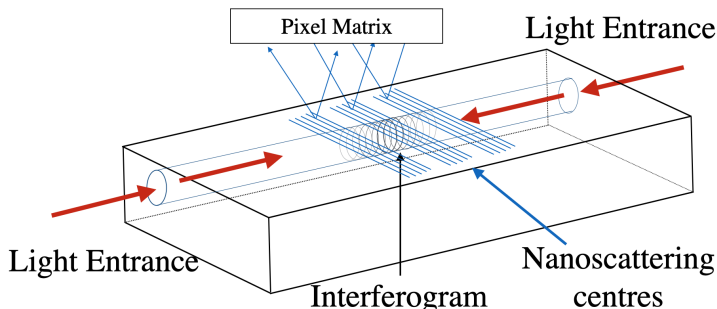


Figure 1. SWIFTS’s principle : the light is injected on both sides of a single mode channel waveguide, extracted by the nano-scattering centres and imaged on the pixel matrix of the detector

A critical aspect of the SWIFTS is the sampling of the wave. Following the Shannon-Nyquist criterion, the interferogram should be sampled with a minimum step of  $\frac{\lambda}{4n}$ , which in this case ( $\lambda = 3.4 \mu\text{m}$  and  $n = 2.14$  for  $LiNbO_3$ ) would mean a pitch between two scattering centres of  $\sim 400\text{nm}$ . This pitch is too small for the actual technologies and ill-adapted to the standard pixel pitch of the mid-Infrared detectors (around  $20 \mu\text{m}$ ) : the signal is undersampled.

This undersampling can be compensated using a spatial and/or a temporal offset. A spatial offset consists in having several parallel waveguides with shifted nano-scattering antennas, and a temporal one would mean using the electro-optical or thermo-optical effects to achieve active modulation of the phase, and therefore scanning the fringes under the antenna, improving the effective sampling step.

### 2.2 Avoiding crosstalk : antennas

In the Mid-Infrared, the effective absorption area of the detectors is buried several hundreds micrometers in a semiconductor layer. Because of this layer, the propagation lengthens, and the radiation pattern of each centre grows wider and wider. This induces crosstalk on the pixels : the signal received by one pixel is a combination of the signals emitted by several scattering centres, without the possibility to discriminate them, hence making the proper reconstruction of the signal impossible.

The solution proposed to avoid crosstalk is the use of the antenna effect : instead of a single one, multiple diffraction nano-grooves are implemented in every scattering centre (antennas), [2] thus creating a small diffraction grating and improving the directivity of each antenna. The chosen number of grooves per centre is 5 [4, 5], as less could result in still having a too wide angular distribution, and more increases the risks of repeatability issues, as well as having too much flux extracted. However, with astrophysical applications in mind, slightly increasing the number of grooves per antenna is still a possibility if the extracted flux is insufficient, while still having to monitor the extraction so that flux remains for the following antennas. (see fig4).

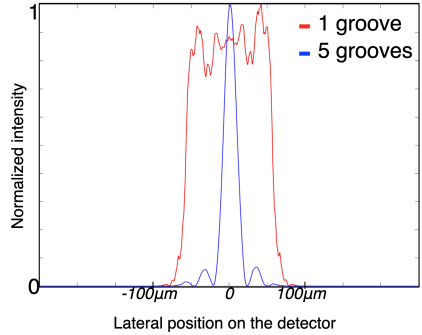


Figure 2. Simulation of the normalised radiation pattern in the sample for an antenna with 1 groove (red) and an antenna with 5 grooves (blue), as recorded by a detector set at X μm from and with a 300 μm active area. The horizontal scale gives the lateral dimension, showing that a high number of grooves allows to reduce the angular divergence. Note that the radiation patterns are normalised, but with 5 grooves the total radiated flux is higher than with only one.

Fig2 shows that the antenna with 5 grooves has a much more directive radiation pattern than the one with only 1 groove : the FWHM goes from ~ 82 μm to ~ 12 μm.

The pitch between two grooves in an antenna should be of  $\frac{\lambda}{n}$ , as this corresponds to the period of the propagative wave. Indeed,  $\frac{\lambda}{n}$  allows each groove to sample the same part of the wave (see fig3). For a typical IR pixel pitch of 20 μm, this means that instead of covering 4-5 pixels with a single groove, all the flux is focused on a single pixel using a 5 grooves antenna. This also allows to increase the number of sampling antenna, without overlapping, thus improving the spectral étendue by reducing the distance between two consecutive sampling centres. As for the pitch between each antenna, it is linked to the size of the pixels of the detector that is used, as each pixel must receive its information from one antenna only. (see fig4) In a first trial sample, this pitch has been set as  $3 \times$  pixel size, in order to ensure that we are avoiding crosstalk.

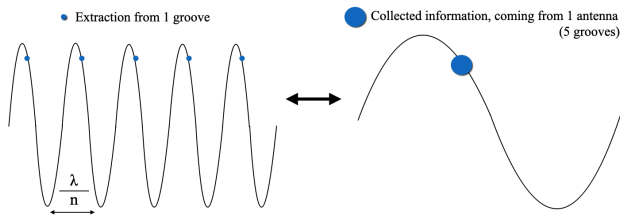


Figure 3. Sampling by 1 antenna composed of 5 grooves : each groove is periodically extracting the signal, and the collected flux on the pixel is a sum of these extractions

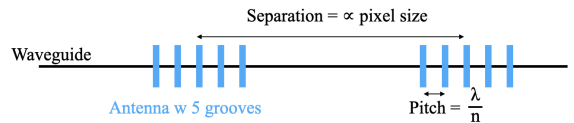


Figure 4. Design of the antennas, with 5 grooves per scattering centre. The pitch between each groove is  $\frac{\lambda}{n}$ , and the pitch between each antenna is determined according to the pixels size.

Fig3, shows that there is still undersampling, as the signal should be sampled at  $\frac{\lambda}{4 \times n}$ . As studied in Section 2.1, this value cannot be obtained directly, however a spatial offset would allow for a better sampling.

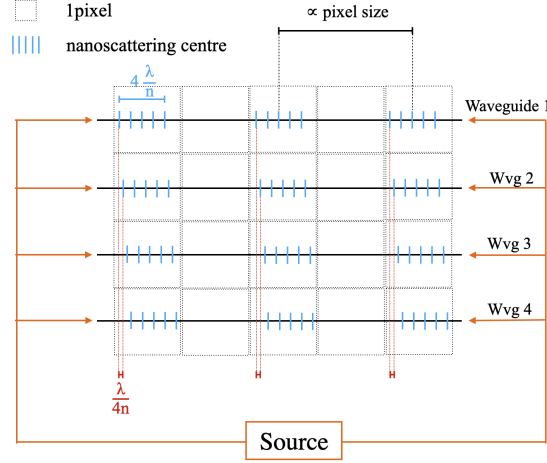


Figure 5. SWIFTS with a spatial offset : there are 4 waveguides, each with a shifted set of antennas. Each antenna has 5 grooves. The light from the source is injected simultaneously in each of the waveguides.

Fig5 represents a top view of a spatially shifted passive SWIFTS; with 5 grooves per scattering centre, and 4 parallel waveguides with shifted antennas. In order to correctly sample the signal, the scattering centres from one waveguide to the other are separated by  $\frac{\lambda}{4n}$ , and within one antenna the grooves are separated by  $\frac{\lambda}{n}$ . Injecting the light from the source simultaneously in all the waveguides allows to sample the wave with the correct pitch. By stitching the collected data on every waveguide, the signal can be reconstructed with a spectral étendue  $N$  times larger than for a single waveguide ( $N$  being the number of shifted channels), and the spectrum of the source can be recovered. However, spatial multiplexing entails a dilution of the incoming flux in  $N$  channels, which diminishes the SNR ratio.

### 2.3 Technologies to make the samples and active modulation of the phase

The first sample is made using a classical lithography technology, with Titane diffusion waveguides and FIB (Focused Ion Beam) antennas. This technology is well-known, and allows for very accurately positioned antennas as well as a precise control on their sizes. The second sample was made using the Direct Laser Writing (DLW) technology, using the depressed cladding index technique to create the waveguides. It involves the transversal inscription of tracks (two dimensional tubular structures) in the regime for Type II index changes. Type II index changes corresponds to a negative index change at the laser writing focal volume, and strong stress field surrounding the track due to lattice amorphization and defect generation, involving collateral piezo-optic index changes [6](#). Finally, each groove is a single track; the antennas were made by simply writing 5 tracks with a separation of  $\frac{\lambda}{n}$ .

The DLW technology presents several advantages. It is a simple and rapid technology, which effectively reduces the fabrication costs. Furthermore, it allows for buried waveguides and antennas. Buried waveguides and antennas make for a more robust sample, as the risk of damaging it while handling it is lessened. Additionally, buried antennas extract the flux in a symmetrical way, as the refractive index is the same on both sides, unlike surface antennas that will radiate more in the sample than out because of the asymmetrical indexes. Moreover, buried waveguides and antennas allow to fabricate 3D designs, opening the way for novel configurations and more and more complex optical paths inside the sample, increasing its robustness and compactness. For instance, multiple input beam combiners for phase-closure studies can be implemented (see ref [7](#) for a 3D-3T example). Finally, DLW is a versatile technology, useful for a wide spectral range, that can be used on a broad variety of materials, such as InfraRed glasses (GLS...) but also electro-optic crystals such as Lithium Niobate.

As mentioned in Section [2.1](#), an active SWIFTS will allow for a better sampling of the wave. For this reason, the samples presented here are made in Lithium Niobate ( $LiNbO_3$ ), an electro-optical crystal.  $LiNbO_3$  has a good transmission in the mid-IR (around 75%), and its electro-optical properties allow for its refractive index to

be locally changed with the application of an electric field (Pockels effect) :

$$\Delta n(E_{app}) = -\frac{1}{2} n(0)^3 r_{33} E_{app},$$

with :  $E_{app}$  = the electric field applied to the sample,  $n(0)$  =  $LiNbO_3$ 's refractive index without any electric field, and  $r_{33}$  =  $LiNbO_3$ 's electro-optical coefficient. Typically,  $r_{33} \sim 30\text{pm/V}$ .

As a change in the refractive index of the material will slightly shift the interferogram, the possibility to finely adjust the index by changing the applied electric field allows for an accurate phase modulation, therefore a better sampling of the wave. A spatially shifted active sample would make for an ideal SWIFTS, however a high voltage value has to be achieved because of the small value of the electro-optical coefficient.

### 3. SWIFTS MID-IR : FIRST RESULTS

#### 3.1 FIB antennas in Titane diffusion waveguides

The waveguides for the first sample were made using Titane diffusion lithography, and the antennas are made using a FIB (Focused Ion Beam). It consists of 50 antenna groups, each separated by  $10\ \mu\text{m}$ , and each composed of 1 groove.

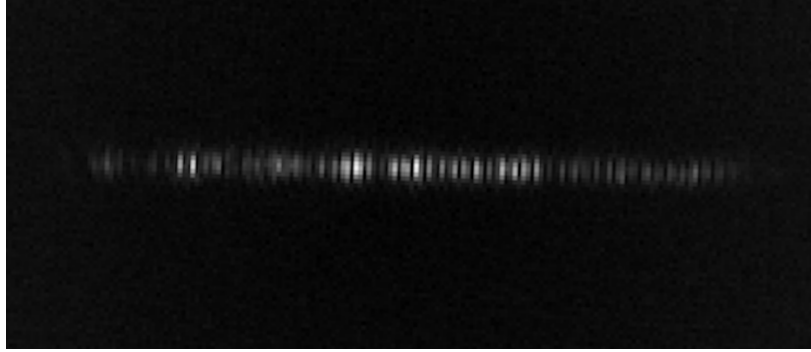


Figure 6. Image of the radiated flux by the FIB antennas on the sample containing 50 antennas (each composed of one groove), with relay optics.

Fig6 shows the obtained results, as seen from above, with relay optics. The waveguides have a good transmission, and the antenna properly extract the light at a wavelength of  $3.39\ \mu\text{m}$ . However, as this configuration was not optimised for the mid-infrared, there is a crosstalk phenomenon (even though it cannot be observed here because of the relay optics). It is due to the fact that only one groove per antenna is not suited to mid-IR detectors, because of its too wide angular distribution. Finally, the antennas themselves are too close to one another to properly separate the flux on the pixel matrix.

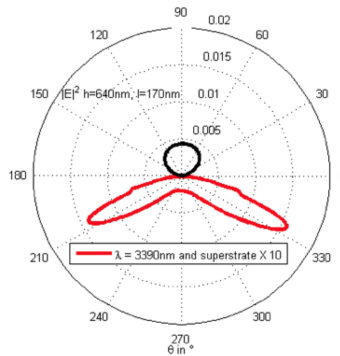


Figure 7. Modelisation of the radiated flux of a surface antenna composed of one groove. Black : upwards radiation, Red : downwards radiation.

Fig7 shows the radiation pattern of a surface antenna composed of only one groove. The flux is asymmetric, both in shape and quantity. The black pattern corresponds to the flux going upwards, outside of the sample, and the red one is the flux going downwards, inside the sample. Because of the difference in the refractive index of the Lithium Niobate and the air, most of the flux is radiated in the sample, and only a small percentage of it goes outwards, which leads to a significant loss in the signal to noise ratio of the spectrometer. This can be avoided by creating buried antennas using the DLW technique.

### 3.2 DLW results

A number of waveguides were made using the depressed cladding index technique, using different parameters in order to study as many configurations as possible. Several tracks (that can be seen on Fig8) are written in the shape of a crown, in order to create a single mode waveguide. Here, the size of the crown is of 30 μm, in order to ensure that it is monomode in the L-band.

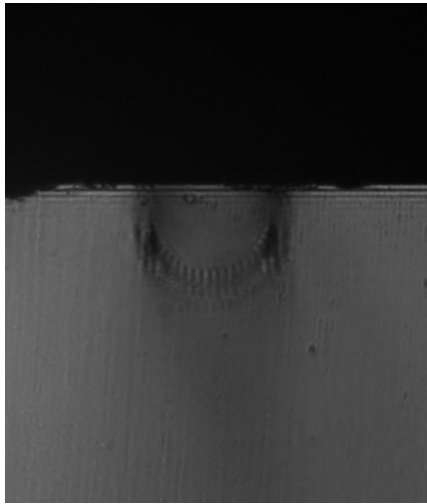


Figure 8. Image in white light of a depressed cladding index waveguide. The tracks creating the 30 μm diameter crown can be seen.



Figure 9. Output of the waveguide, as it is being injected with a 3.39 μm laser

Fig9 shows the output of the same waveguide than on fig8, injected with a 3.39 μm laser. It has a symmetrical output in both the transversal and horizontal ways, and a very good transmission.

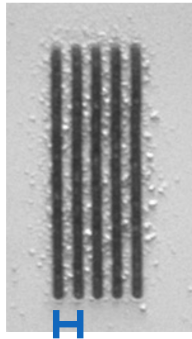


Figure 10. One antenna group, composed of 5 grooves, separated by 3.2 μm

As seen on Fig10, the antennas are composed of 5 grooves, each made by on track, and each separated by 3.2 μm. The ideal separation would have been of 1.6 μm ( $= \frac{\lambda}{n}$ ), however, because of technological reasons, the



pitch between two grooves was doubled. This induces 3 Bragg orders (according to the grating law), but only the first order will be seen on the detector because of total internal reflection.

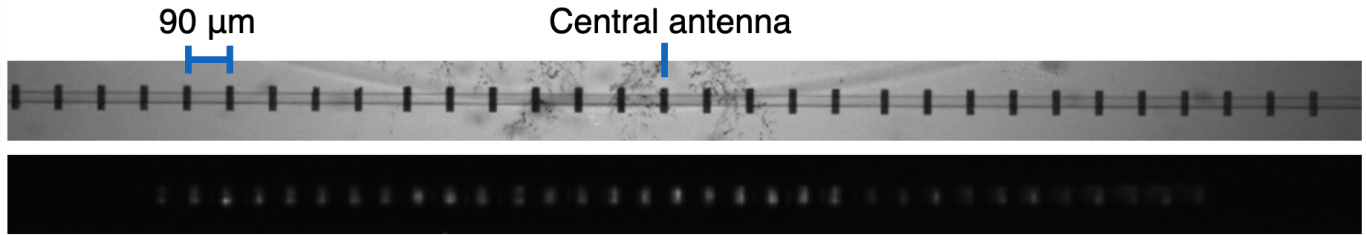


Figure 11. Groups of antennas on the waveguide, in white light (top) and while being injected with a near infra-red laser (bottom)

33 groups of identical antennas were written atop of one of the waveguide, all separated by 90 μm to avoid overlapping on the detector. Each of the antennas is composed of 5 grooves separated by 3.2 μm, and is about 40 μm long (see Fig11 top). The waveguide was injected in the near infra-red, using a 1.55 μm laser. As seen on Fig11 bottom, the antennas are extracting light, and each one of them is perfectly separated. The main points to improve concern the pitch between two consecutive grooves, and the size of the grooves themselves. Fig10 shows that the grooves are about 1.2 μm wide, whereas nanometric grooves were expected. Even though this sample could be optimised, these first results are promising.

### 3.3 Expected signal

Fig 12 and Fig 13 show the simulations that were made to reconstruct the signal that is expected with the samples that were made. These simulations show the result of a waveguide sampled by 20 antennas, with the 10th antenna being the central one, all with 5 grooves separated by 3.2 μm, and each antenna separated by 90 μm. The central antenna is the one where the zero OPD (optical path difference) is obtained : the optical path from each injection is identical.

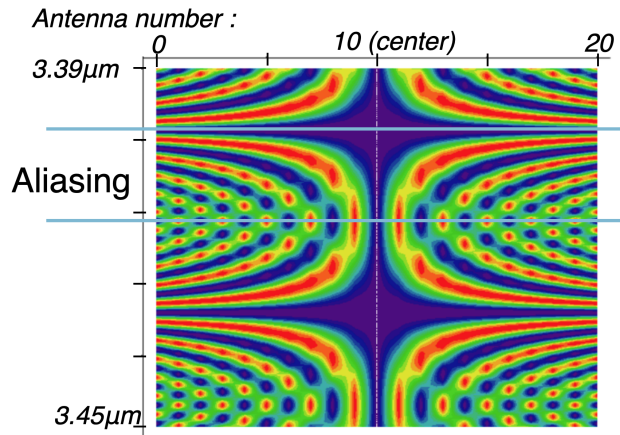


Figure 12. Theoretical sampled signal as a function of the antenna's distance to the centre. The horizontal axis represents the position of the antenna, with the 10th antenna being the central one. The vertical axis represents the wavelength, from 3.39 μm to 3.45 μm. Note that the aliasing window is of 15nm, and can be seen on the pattern.

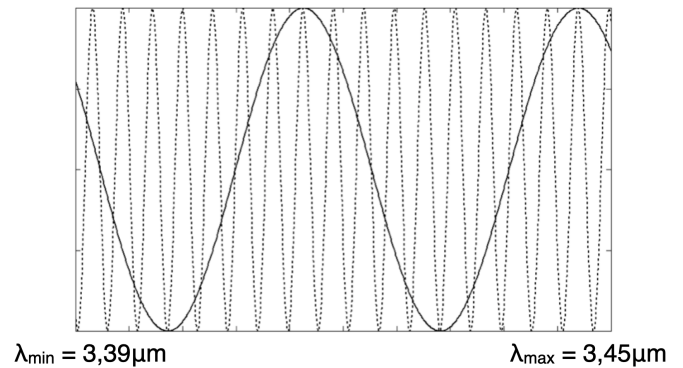


Figure 13. Simulated signal for two antennas, the 11th that is 90 μm from the centre (plain line) and the 20th, 900 μm from the centre (dotted line) for a wavelength range between 3.39 μm and 3.45 μm.

Fig 12 shows that there is a clear non-redundancy window that allows to precisely determine the wavelength as the pattern radiated by the antennas is very distinctive for each wavelength within that window. However, the window is for now smaller than the actual L-band. This is due to the pitch between each antenna group (90  $\mu\text{m}$ ). Reducing this pitch will result in a larger aliasing window, which is what we aim to. This sample is however a first trial, and the antennas were separated quite frankly in order to study precisely the radiated pattern of each antenna. On fig 13 the variation of the response of each antenna according to the wavelength is shown. In plain line, the 11th antenna is represented (90  $\mu\text{m}$  from the centre), and in dotted line the 20th antenna (900  $\mu\text{m}$  from the centre). This figure shows that the further away the antenna is from the centre, the more sensitive it is to small variations in the wavelength. Even with an undersampled signal, the radiation pattern of the antennas could still be used as a high-precision  $\lambda$ -meter [5].

#### 4. CONCLUSION AND PERSPECTIVES

The SWIFTS technology allows for compact, robust, and very high resolution spectrometers (for a 1cm long chip,  $R \geq 10\,000$ ). Implementing a functioning SWIFTS in the L-band (3.4  $\mu\text{m}$  - 4.1  $\mu\text{m}$ ) would be very interesting for a number of astrophysical observations, especially the study of the environment of young stars, and the detection of exo-zodiacal dust. A sample in Lithium Niobate was designed and implemented using the Direct Laser Writing technology, a novel technique allowing for complex buried and 3D-designs. The first results are promising, showing that with optimisations, a mid-infrared SWIFTS could be implemented.

The sample that was made contains many different waveguides and antennas, that need to be characterised in order to completely understand how the signal is extracted. These measurements will be coupled to simulations in order to have a global understanding of the phenomenon.

Finally, a mid-infrared detector will be coupled to the sample, either by means of a pixel matrix glued on the surface of the sample, or by growing the pixel matrix directly on the antennas.

#### ACKNOWLEDGMENTS

The authors acknowledge funding from ASHRA (Action Specificque Haute Resolution Angulaire) 320 from INSU-CNRS and LabEx FOCUS ANR-11-LABX-0013

#### REFERENCES

- [1] E. Le Coarer, S. Blaize, P. B. I. S. A. M. G. L. G. L. P. K. J.-M. F. P. R., “Wavelength-scale stationary-wave integrated fourier transform spectrometry,” *Nature Photonics* (2007).
- [2] Alain Morand, Irene Heras, G. U. E. L. C. P. B. N. C. and Martin, G., “Improving the vertical radiation pattern issued from multiple nano-groove scattering centers acting as an antenna for future integrated optics fourier transform spectrometers in the near ir,” *Optics Letters* **44**, 542–545 (2019).
- [3] de Mengin Fondragon, M., “Étude d’un spectromètre intégré swifts pour réaliser des capteurs optiques fibrés pour les sciences de l’observation,” *Thesis* (2014).
- [4] M. Bonduelle, G. Martin, I. H. P. A. M. C. D. e. a., “Laser written 3d 3t spectro-interferometer: study and optimisation of the laser written nano-antenna,” *Proc. SPIE* (2020).
- [5] Myriam Bonduelle, Irene Heras, A. M. G. U. R. S. N. C. and Martin, G., “Near ir stationary wave fourier transform  $\lambda$  meter in lithium niobate: multiplexing and improving optical sampling using spatially shifted nanogroove antenna,” *Applied Optics* **60**, D83–D92 (2021).
- [6] Huu-Dat Nguyen, Airán Ródenas, J. R. V. d. A. G. M. J. M. M. A. M. C. P. and Díaz, F., “Low-loss 3d-laser-written mid-infrared linbo3 depressed-index cladding waveguides for both te and tm polarizations,” *Optics Express* (2017).
- [7] G. Martin, J. R. Vázquez de Aldana, A. R. C. d. R. S., “Recent results on photonic devices made by laser writing: 3d 3t near ir waveguides, mid-ir spectrometers and electro-optic beam combiners,” *Proc. SPIE* (2016).